Long-range surface plasmons supported by the disordered nanowire metamaterials

Journal:	*Journal of Electromagnetic Waves and Applications*
Manuscript ID	TEWA-2017-0206
Manuscript Type:	Original Article
Keywords:	optics at surfaces, metamaterials, surface plasmons, disorder

Long-range surface plasmons supported by the disordered nanowire metamaterials

Considering the losses of metal and semiconductor and by obtaining exact dispersion relations of the modes, we theoretically study propagation characteristics of surface plasmons supported by disordered nanowire metamaterials. The metamaterials are composed of disordered nanowires made of metal or semiconductor embedded into the dielectric material. In case of the semiconductor nanowires, it is possible to considerably improve the propagation characteristics of surface plasmons supported by the system, as compare to the metallic nanowires.

Keywords: Optics at surfaces, metamaterials.

1. Introduction

Considering the metal and semiconductor losses in the calculations and by obtaining exact dispersion relations of modes, we theoretically study propagation and localization characteristics of surface plasmons supported by the disordered nanowire metamaterials. The metamaterials are composed of the metallic and semiconductor nanowires and dielectric (PbS).

Surface plasmon polaritons (SPPs) offer a promising approach to overcome the diffraction limit of light and to enhance the miniaturization of devices [1]. SPPs have been an attractive and extensively studied topic in scientific community for its various unique features being highly desirable in fields such as highly integrated optical circuits, high sensitive biological sensing, enhancing light-matter interaction, and so on [2, 3]. Recent works include investigations on the generation, propagation, manipulation and detection of light, as well as light-matter interaction mediated by the excitation of SPPs in metal nanostructures [4, 5]. Specifically, SPPs are surface EM waves propagating along the dielectric-metal interface at optical frequencies [6]. Among metamaterial

structures supporting SPPs, one-dimensional metamaterials composed of alternating metal and dielectric layers are the simplest examples [7]. It is possible to treat the heterogeneous material as a homogenized effective medium, whereas local resonances cause exotic values of the effective medium parameters that are found in nature on rare occasions [8].

Since the emergence of the metamaterial research field, the disorder within artificially structured materials has been a subject of extensive discussions [9-11]. Metamaterial at optical frequency can be considered as a kind of man-made architecture material possessing unusual properties [12]. One of its remarkable features is that the equivalent permittivities on different directions differ from each other and can be varied by designing its structure elaborately [12]. It is worthwhile mentioning, that this property enhanced by the presence of the disorder promises that metamaterial may serve for SPP propagating with more flexible performances than conventional metal or ordered metamaterial. For instance, dealing with the photonic crystals, some disorder can dramatically degrade the reflection and transmission properties, which are based on constructive interferences. In contrast, metamaterial media, by taking benefit of strong localization effects is, in theory, not affected by a positional disorder as long as the coupling between these resonators can be avoided [13].

It has recently been shown that the metamaterial interface can support SPPs [14-17]. However the limited number of studies examining the SPPs deals with the disordered metamaterial case. In this paper, considering the losses of metallic and semiconductor nanowires, we examine the propagation characteristics of the SPPs supported by the disordered nanowire metamaterials. Furthermore, we suggest optimal designs of these systems, which are capable of supporting long-range SPPs. To the best of our knowledge, the results presented here have not been reported elsewhere.

2. Dispersive relations and properties of the disordered metamaterials

The structure of the metamaterial is shown in Fig.1, where parameters d and S represent the diameter of the metallic nanowire. All the involved media are nonmagnetic, so the magnetic permeability of every medium is the same as that of vacuum. In our numerical calculation, we use a metallic or semiconductor nanowire metamaterial structure as an example to explore the dispersive features of surface plasmon polaritons, where $\varepsilon_{m,s}^{M}(\omega)=\varepsilon_{\infty}-\frac{\omega_p^2}{\omega^2+i\delta\omega}$. By means of effective medium approximation it is possible to evaluate the effective permittivities of the nanowire metamaterial which are described by the following equations:

$$\varepsilon_{\perp}^{M}=\varepsilon_{d}^{M}\left[\frac{\varepsilon_{m,s}^{M}(1+\rho)+\varepsilon_{d}^{M}(1-\rho)}{\varepsilon_{m,s}^{M}(1-\rho)+\varepsilon_{d}^{M}(1+\rho)}\right] \tag{1}$$

$$\varepsilon_{\parallel}^{M}=\varepsilon_{m,s}^{M}\rho^{M}+\varepsilon_{d}^{M}(1-\rho) \tag{2}$$

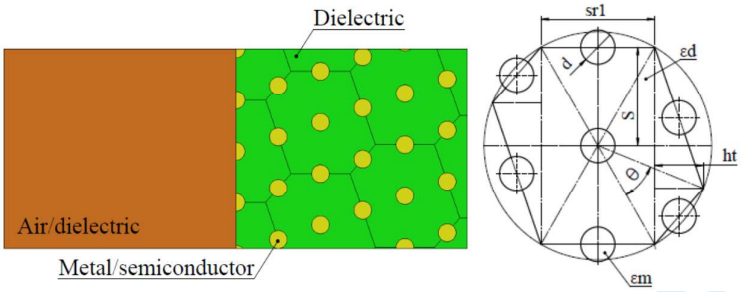

Fig. 1. Fragment of the nanowire metamaterial bounded by the isotropic medium (a) and the corresponding unit cell (b)

Here, subindex M refers to the metamaterial under consideration. Moreover, ρ is the metal fill fraction ratio which is defined as:

$$\rho=\frac{nanowire\ \ area}{unit\ cell\ \ area} \tag{3}$$

A possible way to calculate the metal fill fraction (ρ) is to obtain values for pore diameter (d) and spacing (S) and apply the following equation $\rho = \pi d^2 / \left(2S \cdot \left(ht + sr1\right)\right)$ with ht and $sr1$ being the geometrical parameters of the hexagon in case of irregularly positioned metamaterial (Fig. 1).

It is worthwhile mentioning, that

$$ht = \sqrt{2S^2 + \frac{sr1^2}{2} - 2\left(S^2 + \frac{sr1^2}{4}\right)\cos\theta} \times \sin\left(arc\tan\left(\frac{2S}{sr1}\right) - \frac{\theta}{2}\right) \qquad (4)$$

with θ being the disorder angle (Fig. 1).

Under made assumptions, it is possible to derive the dispersion relation for the surface modes localized at the interface between two media with one being anisotropic. We evaluate the tangential components of the electric and magnetic fields at the interface and obtain a single surface mode with the propagation constant [18]

$$\beta = k\left(-\frac{\varepsilon_d^M \varepsilon_d a\left(\varepsilon_d - \varepsilon_{m,s}^M \rho + \varepsilon_d^M\left(\rho - 1\right)\right)}{b\left(\varepsilon_d^2 + \frac{\varepsilon_d^M\left(\varepsilon_{m,s}^M \rho - \varepsilon_d^M\left(\rho - 1\right)\right)a}{b}\right)}\right)^{1/2}, \qquad (5)$$

Where k is an absolute value of wavevector in vacuum and β is the component of the wavevector parallel to the interface and $a = \varepsilon_d^M\left(\rho - 1\right) - \varepsilon_{m,s}^M\left(\rho + 1\right)$, $b = \varepsilon_d^M\left(\rho + 1\right) - \varepsilon_{m,s}^M\left(\rho - 1\right)$.

3. Results and discussion

In this section, we investigate SPs supported by the metal and semiconductor nanowire metamaterials presented in Fig. 1. In order to obtain a concise insight into the effect of the losses of the metal nanowires on the modes characteristics, we first consider the lossless case. Then, we revise the results by including the losses in the calculations. The parameters of silver are obtained by fitting this dielectric function to a

particular frequency range of bulk dielectric data [19]. It is found [20] that for silver, the values of $\varepsilon_\infty = 5$, $\omega_p = 9.5eV$, $\delta = 0.0987eV$ give a reasonable fit to the bulk dielectric data.It is interesting to notice that heavily doped silicon (n>2.2×10^{19} cm^{-3}) has been shown to exhibit metallic properties at terahertz frequencies [21, 22] and has the potential to replace metals in such applications [23]. The case of a heavy-doped Si is considered, assuming that the doping level is N=5×10^{19} cm^{-3} [24]. Figs. 2-4 show the dispersion curves of the disordered nanowire metamaterial. Although the graphs possess the similar outline with that of traditional metal-SPP, the dispersion curves for the disordered nanowires have some particularities that deserve further considerations.

A. Lossless case

In case the losses are ignored, the plot of Eq. 4 leads to the band structure that can be divided into allowed and forbidden regions. Panels 2 (a), (b) are plotted for different angle θ, i. e. for θ = 10 - 60°. The panel (a) shows the dispersion of the nanowire metamaterial that is bounded with air and the panel (b) – with dielectric (ε=4).

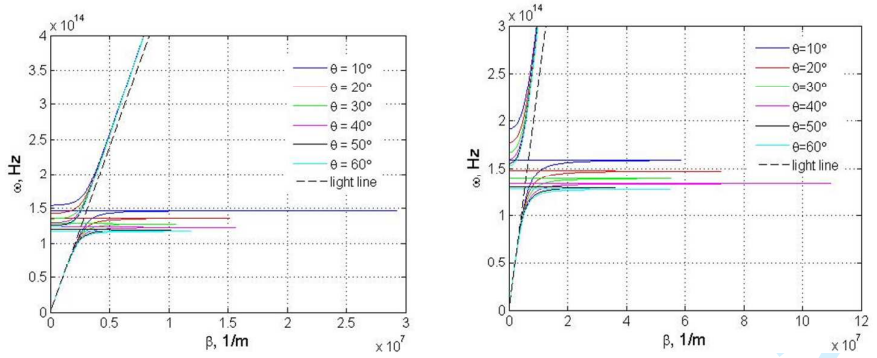

(a) (b)

Fig. 2. The dispersion of SPs supported by the lossless metallic nanowire metamaterial bounded by air (a) and dielectric (b). The black dashed line show the light line.

The allowed modes appear in a wide range of frequency for the specific values of the wavevector β as presented in panel 2 (a), (b). When the metamaterial is bounded with the air, the allowed band shrinks as it is depicted in panel 2 (a). As it is seen from

panels 2 (a), (b), by increasing the angle θ, the SPs supported by the system shifted to lower frequencies; the allowed bands shrink to the narrower regions. It should be mentioned that bands deviate significantly from the light line, and this departure is greater in case of the metamaterial bounded with dielectric. We remark that such dispersion curves exhibited similar behaviors of SPPs propagating along the ordered nanowire metamaterial interface. The asymptotic frequency is tuned by the value of θ, and the maximum value of tuning reaches to 1.6 GHz, if θ=10° and the metamaterial is bound with the dielectric. In the case of the disordered metamaterial, the amendment of θ is equivalent to change in ρ, resulting in the change of asymptotic frequency. For comparison, the dispersion relation of the ordered nanowire metamaterial (θ=60°) is also calculated, as shown in the cyan line in Figs. 2 (a), (b). We observe that the asymptotic frequency of the ordered structure (the cyan line) is lower than that of the disordered structure.

B. Lossy case

Up to now, we have completely ignored the effect of the losses, coming from Re(ε), in our analysis. In the case Im(ε) is involved in the calculations, the wavenumber takes the complex values, i. e. $\beta = \beta' + i\beta''$, and therefore the wavenumber would be complex within the whole frequency region. Panels (a) and (b) of Fig. 3 show the dispersion diagrams and (c) and (d) the propagation length of the surface waves for both cases. While there are visible changes in dispersion curves, the most notable feature is the drastic enhancement of the propagation length as the angle θ is increased.

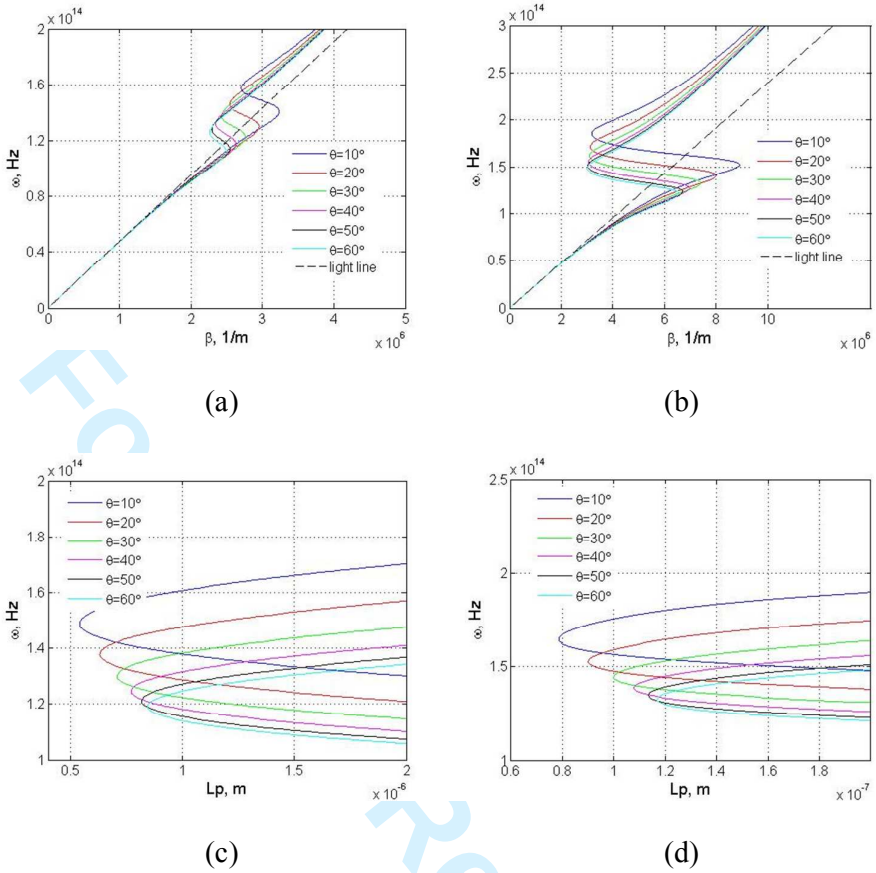

Fig. 3. The dispersion of SPs supported by the lossy metallic nanowire metamaterial bounded by air (a) and dielectric (b) along with the propagation lengths for different cases (panel (a) – air; panel (b) - dielectric); the black dashed line show the light line.

As it is seen from panels (c), (d) of Fig. 3, L_p values of the SPs for θ=60° are considerably smaller than those of θ=10°. This means that when real losses are included, the nanowire metamaterial supports the SPs that are not as efficient as SPs of the disordered metamaterial. By efficient SPs we mean modes with large L_p. From these panels, it can be observed that by decreasing the angle θ from 60 to 10°, the frequency range in which the SPs are supported can be extended. Moreover, the propagation characteristics can also be improved.

Since our goal is to obtain the nanowire metamaterial with the capability of supporting SPs with longer propagation length, for the results presented in Fig. 3 we

have replaced metal with the semiconductor. Figure 4 shows dispersion of the SPs in case of the semiconductor nanowire metamaterial.

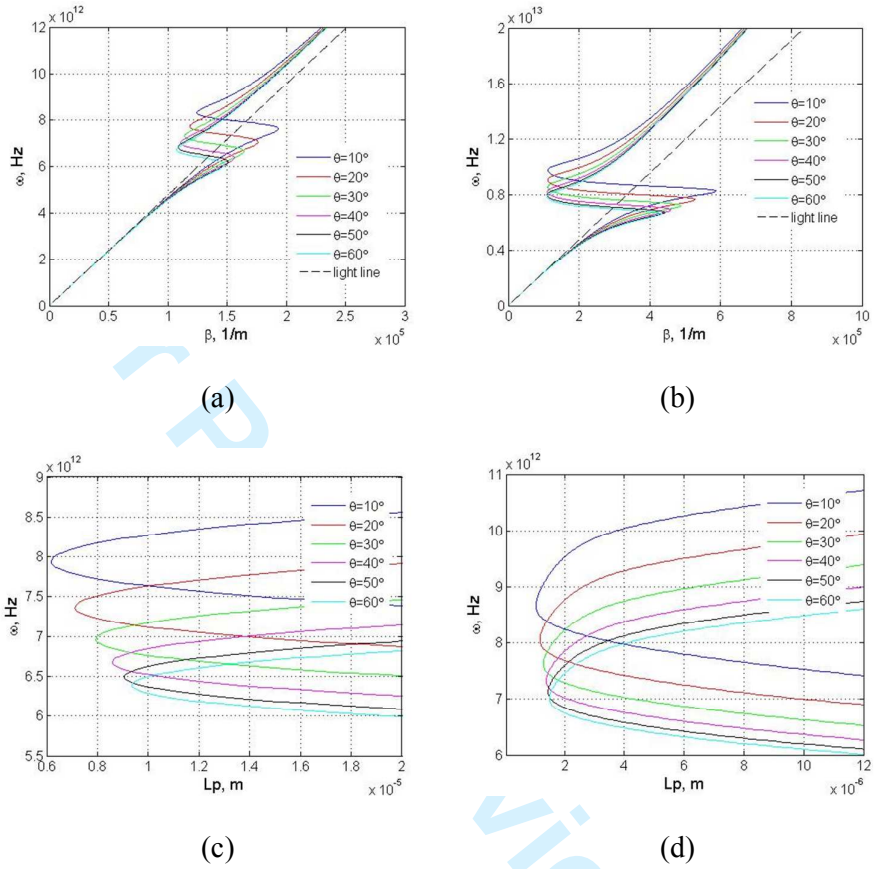

Fig. 4. The dispersion of SPs supported by the lossy semiconductor nanowire metamaterial bounded by air (a) and dielectric (b) along with the propagation lengths for different cases (panel (a) – air; panel (b) - dielectric); the black dashed line show the light line.

It can be concluded that the semiconductor nanowire metamaterials support SPs with the longer propagation length. It is clear that the propagation length of semiconductor-SPPs is around 10 times longer than that of metal-SPP. Thus, the propagation loss of semiconductor-SPPs is much lower than that of metal-SPPs. Consequently, in some circumstances, using the disordered semiconductor nanowire

metamaterial structures would result in longer propagation length. And by adjusting the level of disorder (angle θ), the properties of SPP mode could be tuned.

4. Conclusion

The SPP guided by the disordered nanowire metamaterial was studied theoretically. The dispersion relation of the SPP was derived treating the metamaterial as an anisotropic material by the effective medium theory. It is revealed that semiconductor-SPPs have narrower frequency range than metal. As far as we are concerned, the oscillation of free electrons at the metal surface results with the surface plasmon. Naturally, the decrease of the number of free electrons would lead to the reduction of frequency range. The calculation results also revealed that the semiconductor-SPPs have larger propagation length compared with metal-SPPs. Therefore, at some specific frequency, semiconductors could be more favorable than metal in transmitting signals. Moreover, it should be noticed, that there is a room of possibilities to increase the propagation length of the modes up to two orders by replacing the metallic nanowires with the semiconductor ones. These disordered nanowire metamaterial structures are appropriate for feasibly designing disordered metamaterial, which are beneficial to guiding and sensing applications.

References and links

1. Barnes W. L., Dereux A., Ebbesen T. W. Surface plasmon subwavelength optics. Nature. 2003; 424: 824–830.
2. Zhang D., Zhang Q., Lu Y., Yao Y., Li S., Jiang J., Liu G. L., Liu Q. Peptide functionalized nanoplasmonic sensor for explosive detection. Nano-Micro Lett. 2016; 8(1): 36–43.

3. Zeng S., Sreekanth K. V., Shang J., Yu T., Chen C. et al. Graphene-gold metasurface architectures for ultrasensitive plasmonic biosensing. Adv. Mater. 2015; 27(40): 6163–6169.
4. Lu H., Liu X., Wang L., Gong Y., Mao D. Ultrafast all-optical switching in nanoplasmonic waveguide with Kerr nonlinear resonator. Opt. Express 2011; 19: 2910–2915.
5. Berini P. Surface plasmon photodetectors and their applications. Laser&Photon. Rev. 2014; 8: 197–220.
6. S. A. Maier, Plasmonics: Fundamentals and Applications (Springer: New York, 2007).
7. Gric T. Surface-plasmon-polaritons at the interface of nanostructured metamaterials. Progress in electromagnetics research M (PIER M). 2016; 46: 165-172.
8. Zhang X., Wu Y. Effective medium theory for anisotropic metamaterials. Scientific Reports. 2015; 5: 7892.
9. Nishijima Y., Rosa L., Juodkazis S. Surface plasmon resonances in periodic and random patterns of gold nano-disks for broadband light harvesting. Opt. Express. 2012; 20(10): 11466-11477.
10. Nishijima Y., Khurgin J. B., Rosa L., Fujiwara H., Juodkazis S. Randomization of gold nano-brick arrays: a tool for SERS enhancement. Opt. Express 2013; 21(11): 13502–13514.
11. Moreau A., Cirac C., Mock J. J., Hill R. T., Wang Q., Wiley B. J., Chilkoti A., Smith D. R. Controlled-reflectance surfaces with film-coupled colloidal nanoantennas. Nature. 2012; 492: 86–90.

12. Shekhar P., Atkinson J., Jacob Z. Hyperbolic metamaterials: fundamentals and applications. Nano Convergence. 2014; 1(1): 14.

13. Hao J., Lheurette É., Burgnies L., Okada É., Lippens D. Bandwidth enhancement in disordered metamaterial absorbers. Appl. Phys. Lett. 2014; 105: 081102.

14. Alshits V. I., Lyubimov V. N. Dispersionless surface polaritons in the vicinity of different sections of optically uniaxial crystals. Phys. Solid State 2002; 44: 386.

15. Acuna G., Heucke S. F., Kuchler F., Chen H.-T., Taylor A. J., Kersting R. Surface plasmons in terahertz metamaterials. Opt. Express. 2008; 16(23): 18745-18751.

16. Lockyear M. J., Hibbins A. P., Sambles J. R. Microwave surface-plasmon-like modes on thin metamaterials. Phys. Rev. Lett. 2009; 102: 073901.

17. Hajian H., Caglayan H., Ozbay E. Long-range Tamm surface plasmons supported by graphene-dielectric metamaterials. J. Appl. Phys. 2017; 121: 033101.

18. Iorsh I., Orlov A., Belov P., Kivshar Y. Interface modes in nanostructured metal-dielectric metamaterials. Appl. Phys. Lett. 2011; 99: 151914.

19. Johnson P. B., Christy R. W. Optical constants of the noble metals. Phys. Rev. B. 1972; 6: 4370.

20. Oubre C., Nordlander P. Finite-difference time-domain studies of the optical properties of nanoshell dimers. J. Phys. Chem. B. 2005; 109(20): 10042-10051.

21. Li S., Jadidi M. M., Murphy T. E., Kumar G. Terahertz surface plasmon polaritons on a semiconductor surface structured with periodic V-grooves. Opt. Express. 2013; 21: 7041–7049.

22. Kumar G., Li S., Jadidi M. M., Murphy T. E. Terahertz surface plasmon waveguide based on a one-dimensional array of silicon pillars. New J. Phys. 2013; 15: 085031.

23. Rusina A., Durach M., Nelson K. A., Stockman M. I. Nanoconcentration of terahertz radiation in plasmonic waveguides. Opt. Express. 2008; 16: 18576–18589.

24. Shen L., Chen X., Yang T.-J. Terahertz surface plasmon polaritons on periodically corrugated metal surfaces. Opt. Express. 2008; 16, 3326–3333.